Journal of Laser Applications

RESEARCH ARTICLE | NOVEMBER 02 2023

Modeling and multiobjective optimization of thermal effects of fiber laser cutting of Inconel 600 sheet by employing the ANN and multi-objective PSO algorithm FREE

Mohammad Hossein Razavi Dehkordi; Dheyaa J. Jasim; Ameer H. Al-Rubaye; Mohammad Akbari ✉; Seyed Amin Bagherzadeh; Mohammadreza Ghazi; Hamed Mohammadkarimi

J. Laser Appl. 35, 042060 (2023)
https://doi.org/10.2351/7.0001231

Journal of Laser Applications ARTICLE pubs.aip.org/lia/jla

Modeling and multiobjective optimization of thermal effects of fiber laser cutting of Inconel 600 sheet by employing the ANN and multi-objective PSO algorithm

Cite as: J. Laser Appl. **35**, 042060 (2023); doi: 10.2351/7.0001231
Submitted: 30 August 2023 · Accepted: 13 October 2023 ·
Published Online: 2 November 2023

Mohammad Hossein Razavi Dehkordi,[1,2] Dheyaa J. Jasim,[3] Ameer H. Al-Rubaye,[4] Mohammad Akbari,[1,2,a)] Seyed Amin Bagherzadeh,[1,2] Mohammadreza Ghazi,[1] and Hamed Mohammadkarimi[5]

AFFILIATIONS

[1]Department of Mechanical Engineering, Najafabad Branch, Islamic Azad University, Najafabad, Iran
[2]Aerospace and Energy Conversion Research Center, Najafabad Branch, Islamic Azad University, Najafabad, Iran
[3]Department of Petroleum Engineering, Al-Amarah University College, Maysan, Iraq
[4]Department of Petroleum Engineering, Al-Kitab University, Altun Kupri, Iraq
[5]Department of Aerospace Engineering, Amirkabir University of Technology, Tehran, Iran

[a)]**Author to whom correspondence should be addressed; electronic mail:** m.akbari.g80@gmail.com

ABSTRACT

In this study, the experimental results of fiber laser cutting of Inconel 600 was modeled and optimized by combining artificial neural networks (ANNs) and particle swarm optimization (PSO). The impact of cutting criteria on the temperature adjacent to the cut kerf and roughness of the cutting edge was experimentally evaluated. The independent variables are the cutting speed, focal length, and laser power. The fiber laser cutting characteristics are modeled at different cutting conditions by the ANN method according to the experimental data. The findings indicated that the ANN is performing reasonably well in dealing with the training and test datasets. Also, the multiobjective PSO has been developed to effectively optimize the laser cutting procedure parameters in order to achieve the maximum temperature (the temperature upper than 370 °C) and minimum roughness (lower than 3 μm) simultaneously in order to improve the laser cutting efficiency. Based on the PSO results, the optimal laser power gained at a laser power of 830 and 1080 W at cutting speed ranges from 2 to 4 m/min and maximum focal length ranges between 0.75 and 0.8 mm where the lowest amount of roughness was created. The optimum temperature ranges were between 370 and 419°C. At a laser power of 1000 W and speed of 4 m/min, the smooth cutting edge at minimum roughness was gained without any defects. Transmission of the focal point up to 1.5 mm below the top surface of the sheet improved the roughness of the cutting edge and the cut quality by producing the smooth surface without slags.

Key words: Inconel 600 alloy, laser cutting, particle swarm optimization, artificial neural networks

I. INTRODUCTION

The use of advanced technologies in industries is an inevitable part of the modern manufacturing process.[1] One of the most important things in manufacturing and producing different parts is the need to cut and connect materials to each other.[2,3] Various methods have been used by humans to cut different materials. With the advancement of science and the emergence of new technologies, the use of laser beams for cutting became the focus of scientists and craftsmen around the world. The reason for using these beams to cut different materials is the unique properties of this technology.[4,5] This method is one of the most common and fastest methods used to cut complex geometries.[6] Also, by changing the process parameters and obtaining the optimal parameters, the best cutting quality can be achieved.[7–9] In addition, the use of

devices such as CO_2, Nd:YAG, and fiber laser to cut various materials is very common. In recent years, the need to use metals with high mechanical strength and corrosion resistance at high temperatures has been considered by various industries. One of the most widely used materials in various chemical, marine, and aerospace industries for the manufacture of a high-pressure equipment is Inconel 625.[10,11] Therefore, the use of laser technology for cutting, due to the difficult working conditions for this type of metal, is a suitable method.[12] Also, to achieve a standard and appropriate cut, the use of numerical methods can be very suitable along with experimental methods. One of the numerical methods that has become popular among researchers in recent years is the use of artificial neural networks (ANNs).[13–16] ANN modeling and multi-objective manufacturing process optimization is a potent and effective method for addressing complex production issues.[17–19] Because they can use input data from a range of sources, such as production time, energy usage, material cost, and quality, ANNs have an advantage in that they can use these input data to forecast outcomes and optimize the manufacturing process. ANNs are excellent for manufacturing optimization because they can recognize patterns in data and adjust to changing circumstances. Manufacturers can optimize their production process with the help of ANNs to increase productivity and cut expenses. Furthermore, by maximizing the process to produce the highest overall performance, ANNs can be utilized to balance opposing goals, such quality and cost.[20–22] In addition, machine learning and model-based optimization have grown in importance as techniques for optimizing the effectiveness of the manufacturing process.[23–25] Manufacturers may evaluate their data and develop models that anticipate the best method to produce items, from improving the production process to predicting output quality, by applying machine learning algorithms. Manufacturers may improve their processes depending on a variety of factors, including cost, quality, and speed, using multi-objective optimization. Manufacturers can locate production bottlenecks, choose the best production processes, and increase productivity by combining machine learning and optimization approaches. Manufacturers can develop a production process that is more productive and economical with the use of machine learning.[26–29] Roy *et al.*[30] studied the cutting quality of laser on Inconel 625 super alloy in different environments. Their results showed that laser power is the most sensitive controllable variable for cutting depth. Sensitivity analysis also showed that the depth is more sensitive with higher air pressure while it is negatively sensitive with water column height. Shrivastava *et al.*[31] predicted and evaluated the optimal cutting quality of the Inconel 718 sheet using different numerical methods. By developing the ANN method and using genetic algorithms and particle swarm optimization techniques, they introduced the optimal parameters of the process to achieve an ideal cut. Vagheesan *et al.*[32] obtained the optimal parameters of the laser cutting process using an ANN-genetic algorithm and ANN–particle swarm optimization (PSO) hybrid modeling. The results showed that the combined model ANN-GA and ANN-PSO is an efficient tool for optimizing process parameters in laser cutting. It was also found that the ANN-GA hybrid model is very useful to obtain the kerf width, kerf taper, and minimum roughness. Using a numerical simulation based on regression, Shrivastava *et al.*[33] obtained the optimal parameters of the Inconel 718 alloy laser cutting process. The results showed that by comparing the optimal process parameters with the experimental results, high quality cutting can be achieved. Chaki *et al.*[34] performed multivariate optimization for optimal parameters of the laser cutting process using the ANN-NSGAII model. The results showed that the prediction accuracy of the ANN module was very good. By comparing the results with the optimized experimental results, only less than 1% error was observed. In a numerical study, Roy *et al.*[35] analyzed the sensitivity of parameters affecting the cutting quality of the Inconel 625 alloy laser. The results showed that all Nd: YAG laser parameters can affect the cutting width, and the sensitivity effect of pulse frequency and cutting speed parameters is less than laser power. Roy *et al.*[36] in an experimental study evaluated the quality of laser cutting on the Inconel 625 alloy. Their results showed that the use of appropriate parameters in the laser cutting process can improve the quality of the cut. Wei *et al.*[37] examined the cutting kerf size and microstructure of the cutting area on the Inconel 738 superalloy in the femtosecond laser cutting process. The results showed that Defocus is a key parameter in cut kerf size. Also, changing the scan speed can lead to changes in the microstructures of the cutting region. Jafarian *et al.*[38] conducted studies to evaluate the hardness and roughness of the surface of the Inconel 718 alloy in the laser cutting process. They investigated the laser cutting parameters using experimental studies and an ANN model. The results showed that the use of this model can lead to increased cutting accuracy as well as the appropriate quality of kerf width and surface roughness. Tebassi *et al.*[39] used the ANN method and the response surface (RSM) method to model the surface roughness and cutting force on the Inconel 718 super alloy. Their results showed that the use of ANN compared to RSM is a reliable, accurate, and better method for predicting and detecting nonlinear mathematical models of surface roughness and cutting force in terms of correlation and error. Nukman *et al.*[40] performed laser cutting optimization using an artificial neural network model. The experimental data of the Taguchi L9 orthogonal array were used to train the ANN model. The simulation results showed that due to the advantages of the developed GA-Taguchi ANN model in manufacturing processes, the maximum prediction error can be reduced below 10%. Grepl *et al.*[41] investigated the effect of process parameters on laser cutting of the Inconel 625 alloy. The results showed that increasing the inert gas pressure, reducing the nozzle distance to the workpiece surface, and decreasing the speed of laser can lead to an increase in the spot radius of the beam. Using multiple regression analysis (MRA) and ANN, Radovanović *et al.*[42] performed an adaptive modeling for the CO_2 laser cutting process. By comparing the experimental results and the predictions of the models, it was found that the ANN model provides more accurate predictions compared to the MRA model. Using a Taguchi-artificial neural network hybrid numerical model, Yang *et al.*[43] introduced a predictive model of the CO_2 laser cutting process. The results showed that the artificial neural network has good capability and accuracy in predicting the laser cutting process. Also, the use of the Taguchi method is very accurate in some cases and regions near the Taguchi control points. Using an ANN model, Tsai *et al.*[44] obtained the optimal laser cutting parameters for QFN packages. The results showed that the ANN model has a good ability to predict the laser cutting quality of QFN packages. It

was also found that using the optimal parameters, the width of the heat affected zone is reduced. There are some studies that used the hybrid approach of ANN and combination of PSO and other optimization algorithm to model and optimize the laser cutting process. Pramanik *et al.*[45] investigated low-power fiber laser cutting of titanium alloy using particle swarm optimization methods. The quality characteristics including kerf taper and heat-affected zone were considered the responses according to utilizing the laser sawing strategy.

Chaki *et al.* evaluated the efficiency of entropy-based ANN-PSO model for optimization of cutting quality in pulsed Nd:YAG laser cutting of aluminum alloy. The kerf width, kerf deviation, surface roughness, and material removal rate were output parameters. The prediction accuracy of the ANN module and the optimized output was about 1.74% error and less than 2% error, respectively.[46] Shrivastava *et al.*[47] developed a prediction model for Nd:YAG laser cutting to achieve better cutting quality, precision, and geometrical accuracy using the artificial neural network technique. These predicted models have been optimized using a multi-objective genetic algorithm and particle swarm optimization techniques, in order to ascertain the optimal range of cutting parameters.

This research was conducted to effectively model the impact of fiber laser cutting measures on cutting region temperature and roughness of cutting edge of the Inconel 600 alloy sheet. Then based on the PSO algorithm, the independent variables (e.g., cutting speed, focal length, and power) were chose to achieve the lowest roughness and highest temperature during laser cutting of the Inconel 600 sheet.

II. MATERIALS AND METHODS

A. Experimental setup

A 3 axis laser cutting Computer Numerical Control (CNC) equipped with a single module fiber laser source with the highest output power of 1500 W and Raytools autofocus BM109 cutting head was employed for cutting tests. For the cutting procedure, oxygen gas at a pressure of 8 MPa and 99% purification through a copper nozzle was employed. K-type thermocouples were utilized at a distance of 2 mm from the center of the cut kerf region to measure the temperature at two different locations. The thermocouples' signal is transformed to the temperature via the Advantech USB4718-module and LabVIEW developed software. The material utilized for cutting was Inconel 600 with 1.5 mm thickness. The Olympus SZX-18 stereoscope was applied to provide the striation pattern of the cutting edge. A 3 axis HS-GB-22EQ CNC machine was employed for cutting procedures. A Mahr Perthometer M2 was applied to analyze the cutting edge surfaces roughness.

B. Laser cutting experiments

To determine the impact of cutting parameters on the quality of the cutting edge and the cutting region's temperature, laser cutting tests were undertaken. Before executing the main set of experiments, a series of preliminary experiments was performed to select the main parameters' level limitations. The laser cutting parameters' levels are provided in Table I.

TABLE I. Laser cutting parameters' levels selection.

Parameters	Levels
Cutting speed (m/min)	2–10
Focal length (mm)	0.4–0.8
Power (W)	800–1200

Generally, measuring the temperature during cutting can give a clear threshold level for parameters' selection in order to evaluate the cut quality indirectly at lower cost and time. Then, based on the provided results from the experiment, the ANN method can develop a highly economic and cost-effective way to predict the cut quality. Measuring the temperature not only evaluate cutting condition but also give a quantitative criterion to select the cutting parameters at the appropriate region. For cutting of Inconel 600, the temperature below 340 °C resulted in incomplete cut kerf and creation of some slags at the cutting edge. High level of temperature resulted in burning corners, wide kerf, and even rough striations at cutting edge due to experiencing excessive heating cycles. Seemingly, the appropriate temperature during the cutting process can effectively monitor the cutting condition, and thereby, it could be useful to evaluate the cut quality with suitable precision. A schematic and actual vision of the laser cutting tests is observed in Fig. 1. The thermocouples were attached at the bottom surface of the Inconel 600 sheet, and the temperature near the cutting region was measured by the thermocouples via USB 4718 and LabVIEW software. Generally, the temperature is measured from the bottom surface of the Inconel 600 sheet where the nozzle tip of the laser cutting head has not any limitation for cutting and collision with the thermocouple tip. Some grooved were engraved at the bottom surface of the sheet up to 0.8 mm thickness to locate the thermocouples. The laser beam location has had a distance of 2 mm from the thermocouple tip from the top surface as shown in Fig. 1(b). Then the thermocouple signal transmitted to the USB4718 module to grab and process by LabVIEW software. Before executing the laser cutting experiments, all thermocouples were calibrated at the ranges between 0 and 200 °C with the maximum error of 1% in the measurement range.

Additionally, Table II illustrates all selected parameters to effectively assess the impact of cutting parameters on heat near the cutting zone and roughness of the cutting edge. Also, Table II enumerates the input and output parameters that were considered in the training process of the ANN. In this research, 21 experiments were done to examine the effect of cutting parameters on cutting zone heat and cutting edge roughness. The independent variables were the cutting speed, focal length, and power, while the dependent variables were the maximum temperature and minimum roughness. The cutting velocity was varied between 2 and 10 m/min, while the power ranged from 700 to 1200 W, and the focal length was in the interval between 0.4 and 0.8 mm. The aim of the study was to minimize both temperature and roughness, with a minimum temperature threshold of 370 °C.

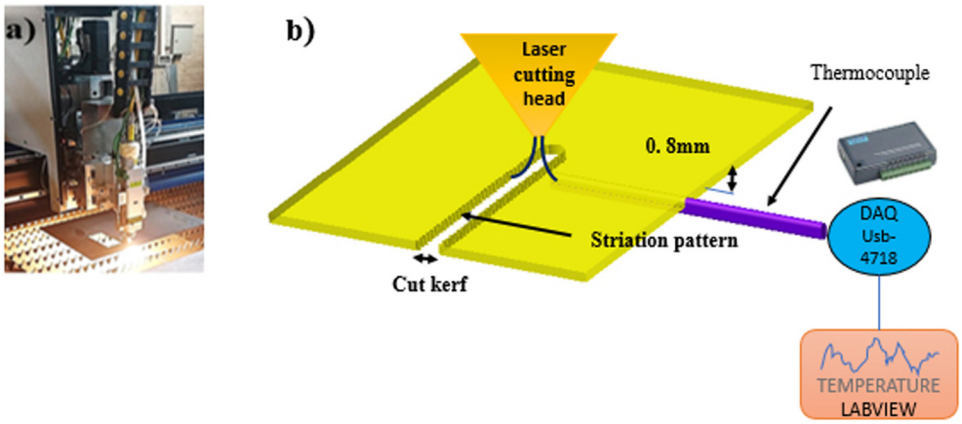

FIG. 1. Laser cutting experimental setup: (a) Actual view; (b) schematic vision.

1. Cutting parameters' impact on the cutting edge state

The outcomes of the experiments are presented to evaluate the impacts of cutting velocity, focal length laser, and power on the cutting edge state. Thus, the SEM images from the cutting edge section were provided to evaluate the impact of cutting situation on cutting edge quality. Figure 2 illustrates the influence of cutting velocity on the cutting edge situation. At light level cutting velocity [Fig. 2(a)], some dross attachment at the bottom side of the cutting edge was observed. Additionally, due to the accumulation of laser heating, the volume of melted materials increased more than optimal cutting condition, and the cutting edge surface seems to be more rough. At optimum cutting speed [see Fig. 2(b)], the cutting edge surface seems to be smooth, and no slags or dross is observed. At high cutting speed [see Fig 2(c)], the striation lines are not straight and seems to be thicker than optimum condition. Moreover, some slags are observed at the bottom of the cutting edge, which, in turn, increase the average cutting edge measured roughness.

TABLE II. Inputs and outputs of test findings.

Test number	Cutting speed (m/min)	Max. temperature (°C)	Focal length (mm)	Power (W)	Roughness (μm)
1	8	255	0.7	800	4.98
2	8	390	0.5	1000	3.12
3	4	355	0.7	800	3.31
4	4	470	0.7	1000	2.61
5	4	510	0.5	1000	2.45
6	6	440	0.4	900	2.85
7	6	339	0.8	900	3.41
8	10	246	0.6	900	5.11
9	4	410	0.5	800	4.82
10	2	470	0.6	900	2.58
11	6	390	0.6	900	2.98
12	8	315	0.7	1000	4.68
13	8	300	0.5	800	4.83
14	6	317	0.6	700	3.85
15	6	458	0.6	1100	2.68
16	10	232	0.6	1000	5.25
17	10	274	0.6	1200	4.91
18	10	208	0.6	800	5.34
19	4	540	0.5	1200	2.35
20	4	320	0.8	1200	3.48
21	4	387	0.7	1200	3.15

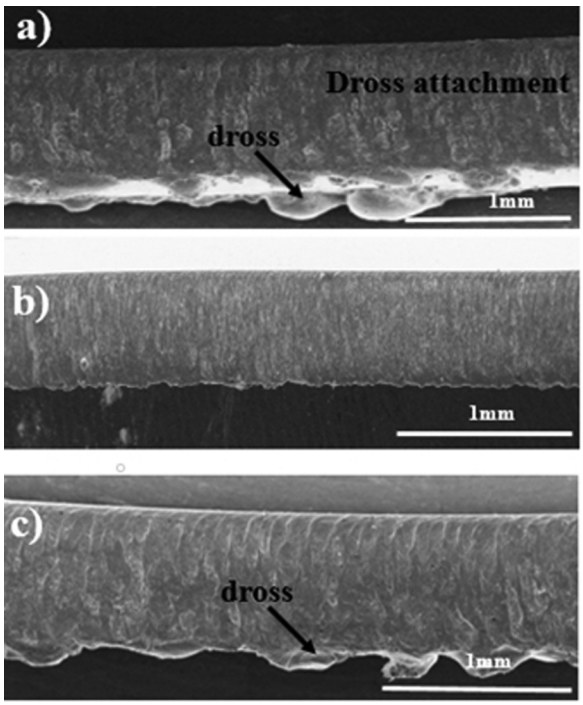

FIG. 2. The impact of cutting velocity on the striation pattern at 1000 W and focal length of 0.5 mm for cutting velocity of (a) 4, (b) 8, and (c) 10 m/min.

Generally, selection of laser cutting velocity and power is highly depending on each other. Commonly, highest cutting is selected according to highest level of the laser source power.

As it is seen in Fig. 3, the impact of power levels has been evaluated on the cutting edge quality condition. As shown in Fig. 3(a), at a low power level of 800, due to having insufficient laser beam energy, there is no clear striation pattern at the cutting edge, and many slags are viewed at the bottom side of the cutting edge. Hence, due to having uncompleted melting of the materials at the cut kerf, most of the melted material at the upper side of the edge have been solidified at the lower side of the edge and formed slags along the cut kerf. At laser power of 1000 W [see Fig. 3(b)], the smooth cutting edge with the straight striation pattern is observed without any slags or dross. This cutting condition leads to minimum roughness in comparison to other conditions. At higher level of laser power of 1200 W, the striation pattern seems to be thicker than 1000 W. On the other hand, some attached dross is observed at the bottom side of the cutting edge. Therefore, it leads to the maximum roughness of the edge.

Generally, the focal point assesses the position of the maximum energy level of the beam for the laser cutting procedure. By changing the focal point condition from the top side of the sheet to the bottom side, the striation pattern at the material thickness according to the changes in the materials flow from the laminar layer to the turbulent flow altered the cutting. Figure 4(a) illustrates the cutting edge condition when the focal point position has a distance of −1 mm below the top surface of the sheet. Below the focal point because of having the turbulent flow and lower energy density, the melting efficiency has reduced and some cavities created at the region of the bottom surface of the sheet. Furthermore, the back-flow rate of the melted materials adjacent to the kerf wall has influenced the striation pattern of the cutting edge from straight to the curvy lines. Figure 4(b) implies on the focal point situation of −1.5 mm from the sheet top side (the focal point located at the bottom of the sheet). Due to having highest level energy density along the sheet thickness, the material flow rate has been uniform and thereby smooth cutting edge surface created without any dross formation or defects. Figure 4(c) shows the appearance of the cutting edge when the laser beam focal point located at the top surface of the sheet. In this case, attached slags are explicitly viewed at the bottom side of the cutting edge, and the striation lines have been significantly deviated from the straight path of the cutting kerf wall. Therefore, insufficient level of beam energy transformed the melted material flow direction and a considerable of solidified dross attached to the bottom of the cutting edge.

III. ARTIFICIAL NEURAL NETWORK MODEL

As mentioned earlier, there are three continuous variables as predictors, namely, the cutting velocity, focal length, and power. Also, the maximum heat and roughness are the outputs evaluated by the tests. Only 21 experiments are conducted due to the limited

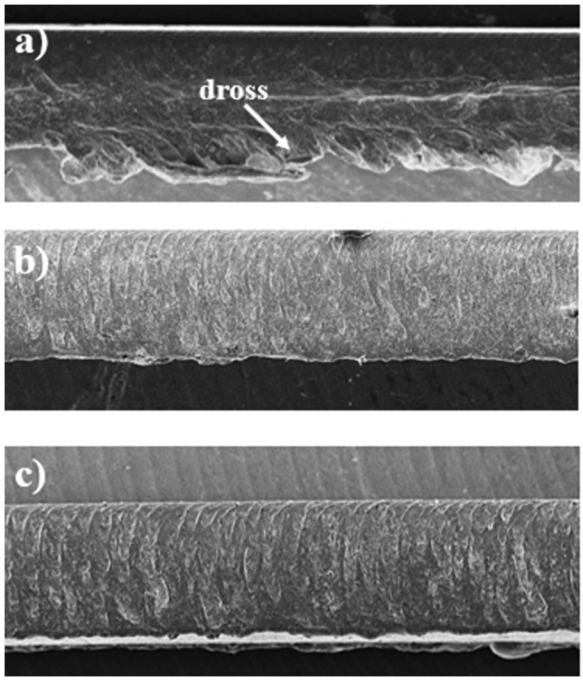

FIG. 3. The impact of power on the striation pattern at 4 m/min and focal length of 0.5 mm and power of (a) 800, (b) 1000, and (c) 1200 W.

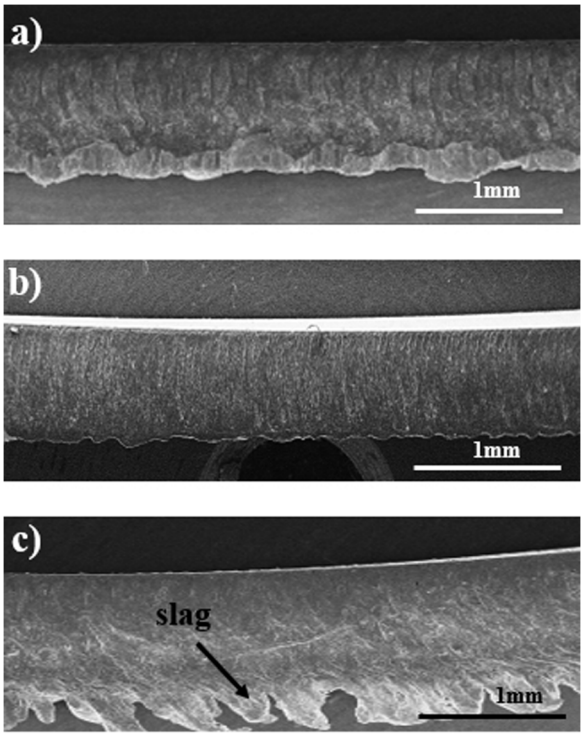

FIG. 4. The impact of laser focal length on the striation pattern at 1000 W, 4 m/min and focal length distance from top side at (a) −1, (b) −1.5, and (c) 0 mm.

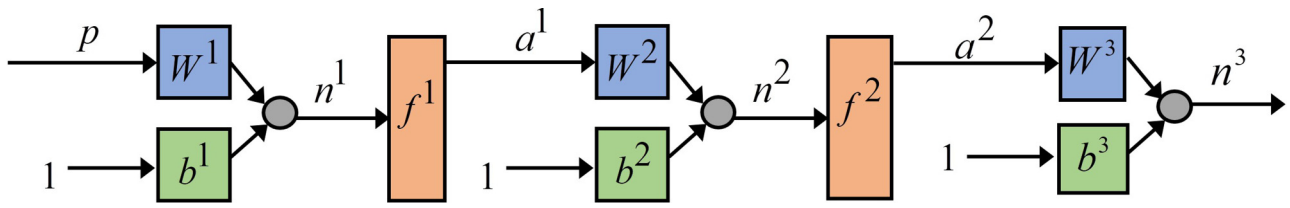

FIG. 5. A schematic slight of the ANN architecture.

time and cost. Therefore, a regression method is needed to interpolate between the conducted experiments. An ANN model is used for this purpose. The ANN has two hidden "tansig" layers and one "purelin" output layer. The number of hidden neurons is determined by trying out all possible numbers and finding the MSE between the outputs and targets. The number of hidden neurons that corresponds to the minimized average MSE is selected. In this research, the number of hidden neurons is 17 and 9. There are two models with three inputs and one output. The "trainbr" method is utilized for supervised learning. A schematic slight of the ANN architecture is demonstrated in Fig. 5.

In Fig. 6, the ANN training performance graphs for the maximum temperature and roughness are plotted. These graphs show the MSE values for not only training but also test datasets over the training iterations (i.e., epochs). The graphs illustrate how well the ANN is performing during the training process. Based on the results, the ANN converges to a minimum MSE value, and the training is halted to prevent overfitting.

Figure 7 illustrates the regression plots for the maximum temperature and roughness. The plots show the outputs plotted against the targets for both training and test datasets. This type of plot is a common way to visualize the performance of the ANN. In a good regression plot, the data points should be close to the diagonal line, which represents a perfect match between the targets and the outputs. The nearest the data points are to the line, the better the model's performance. In this case, the plots show that the ANN is performing reasonably well, with most of the data points clustered close to the diagonal line. However, there are also some points that are further away from the line, indicating that the model is not perfect and there is room for improvement.

As shown in Fig. 8, the error histograms of the ANN represent the distribution of errors between the predicted outputs and the actual targets for both the training and test datasets. These histograms provide insight into the accuracy and consistency of the ANN model in predicting the target variables. A well-performing model would have error histograms that are centered around zero and have relatively low variance, indicating that the predicted values are adjacent to the real values. As can be seen, the error distribution is acceptable in this case.

Figures 9 and 10 depicted the results of the trained ANNs. The maximum temperature and roughness are plotted for dissimilar values of the cutting velocity, focal length, and power.

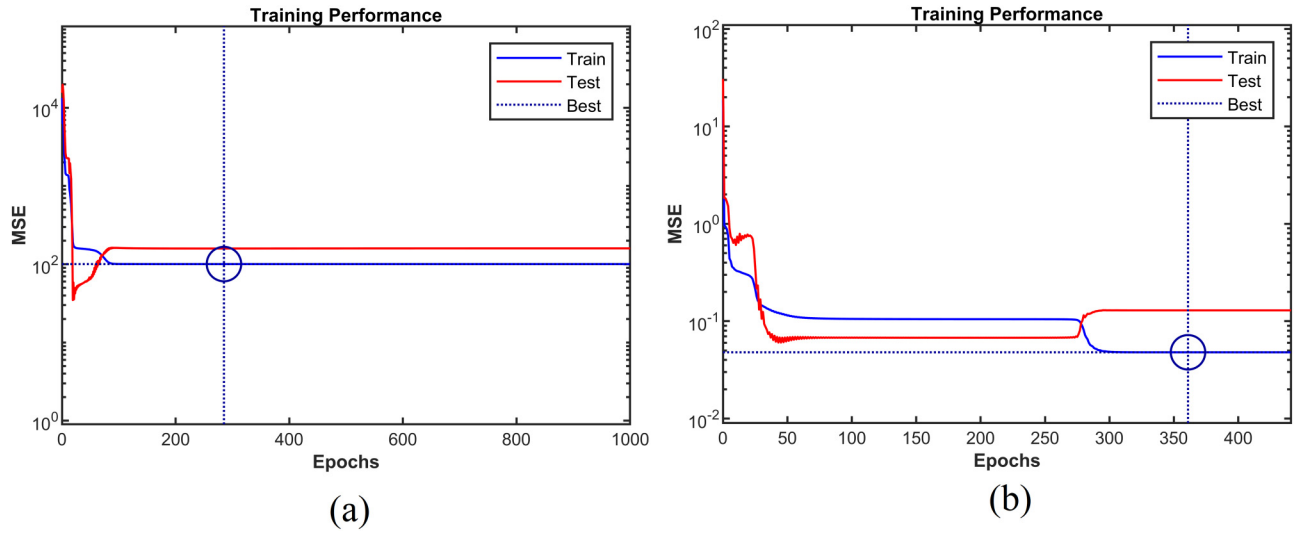

FIG. 6. The ANN training performance graphs for (a) the maximum temperature and (b) roughness.

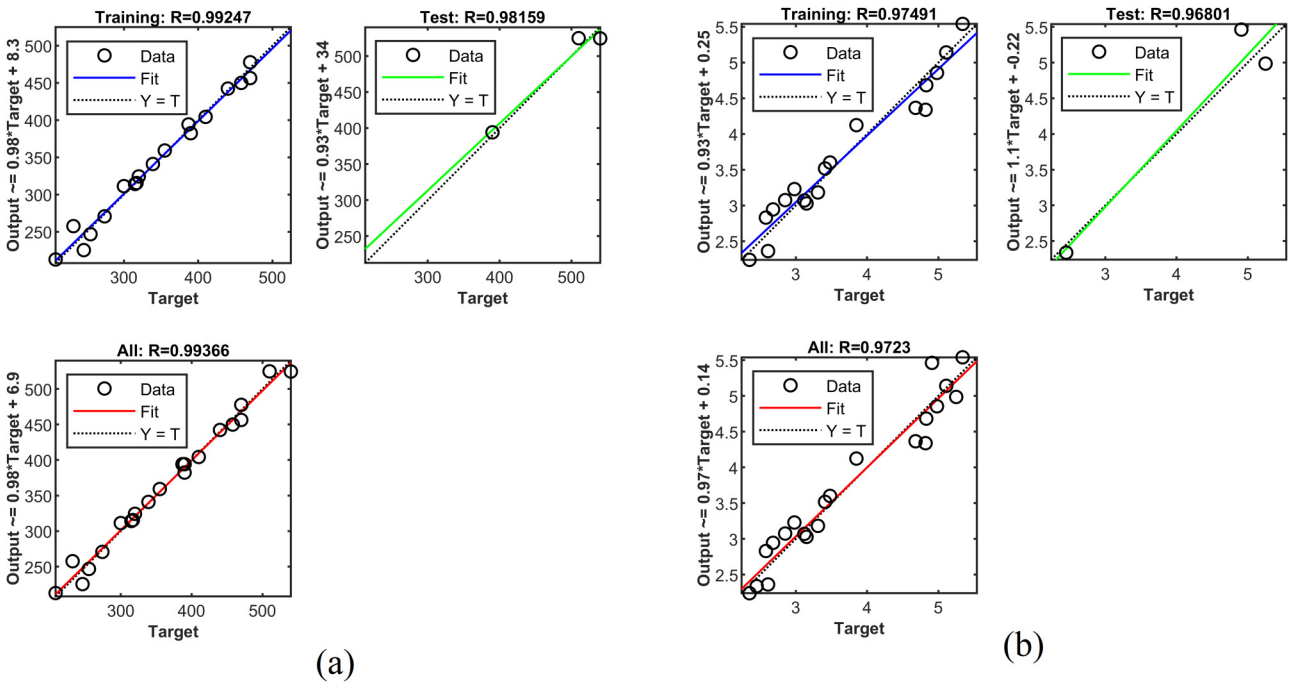

FIG. 7. The regression plots for (a) the maximum temperature and (b) roughness.

IV. PSO OPTIMIZATION ALGORITHM

In the presented part, the multiobjective PSO optimization algorithm is described. Also, the usage of the PSO algorithm for optimizing the fiber laser cutting characteristics of the Inconel 600 alloy is investigated.

A. Motivation

A flock of birds that are in motion over an area must find a point for landing. In this situation, determining the point where all the birds should land is a complex problem because the answer depends on various factors such as the available

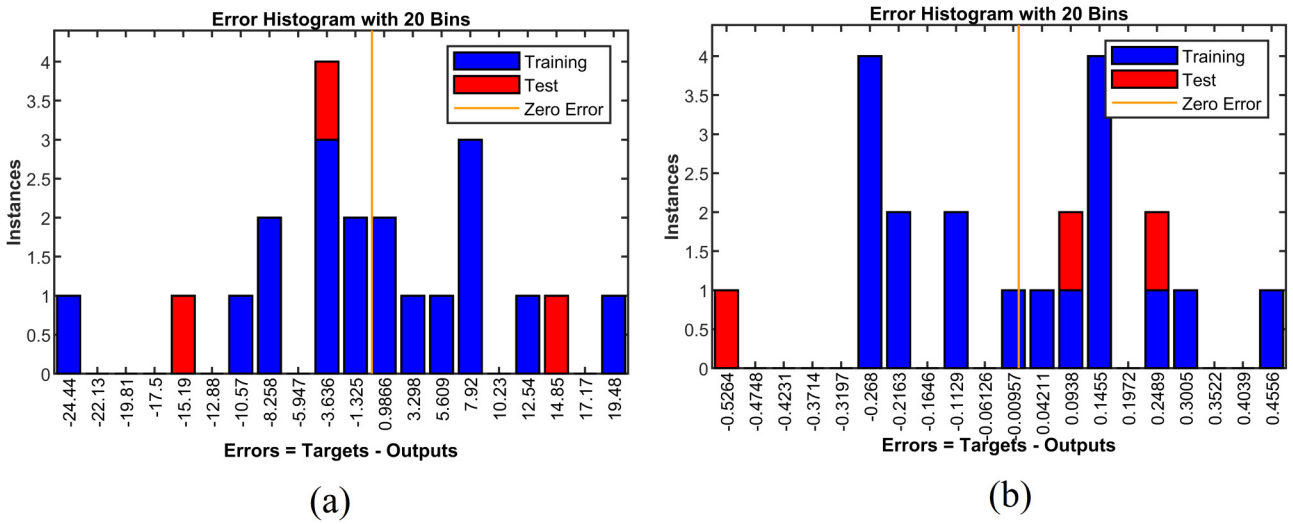

FIG. 8. The error histograms for (a) the maximum temperature and (b) roughness.

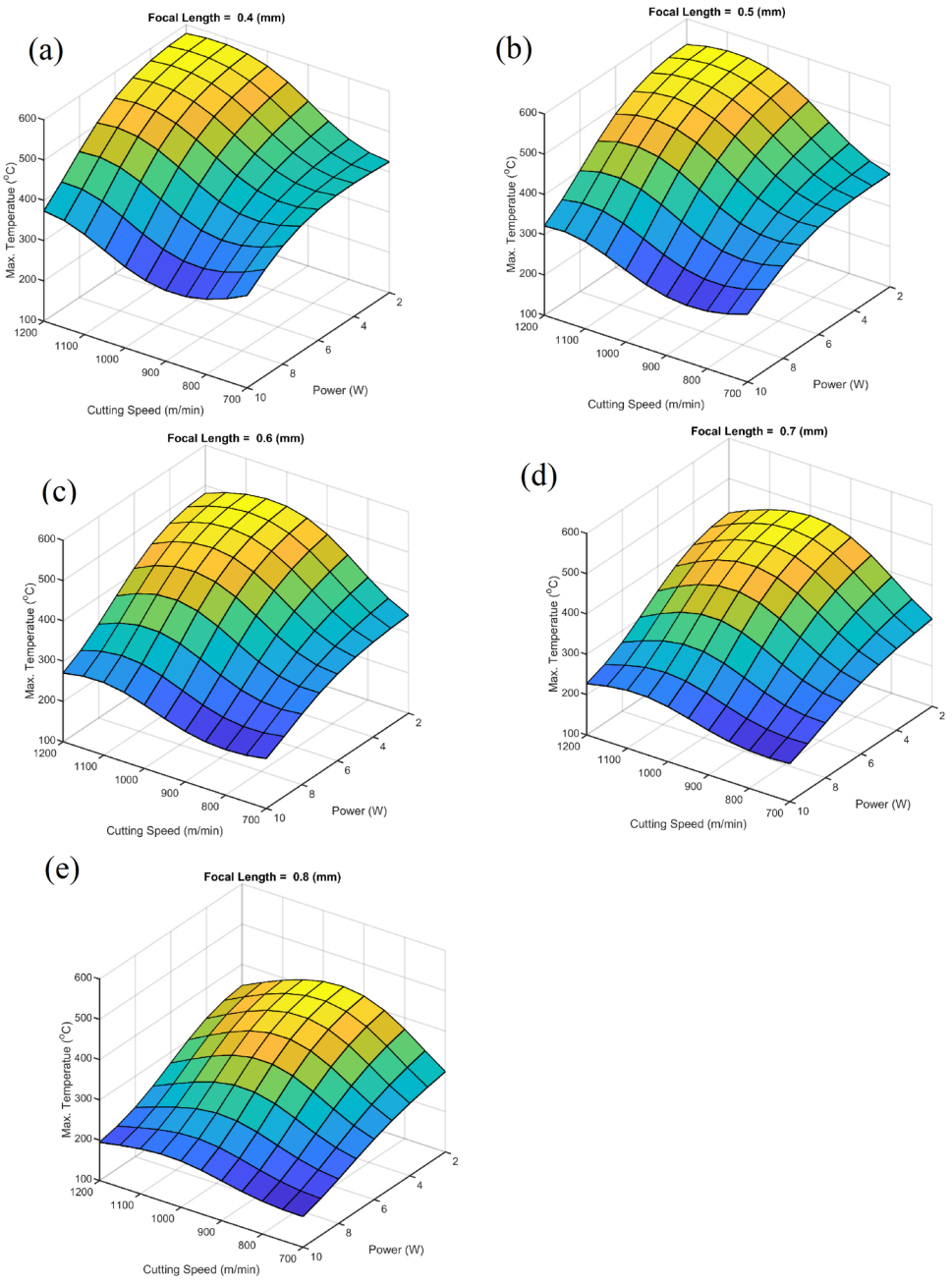

FIG. 9. The highest temperature for the focal length of (a) 0.4, (b) 0.5, (c) 0.6, (d) 0.7, and (e) 0.8 mm.

food resources, the risk of predators at the landing point, the distance to the target landing site, the terrain features, the wind conditions, and any other relevant factors. The birds move simultaneously for a period of time to determine the best place to land, and the whole group lands simultaneously. Research on bird behavior indicates that all birds in a flock that are looking for a good landing point are able to become aware of the best landing point when it is found by one of the members of the flock. Using this awareness, each member of this flock balances their "personal experience" and "social knowledge." Finding the best landing point is an optimization problem. They would need to come up with a method for optimizing the objective function. The group would also need to consider any constraints or limitations that could affect the landing. They would need to test their landing strategy to ensure that it is safe and effective.

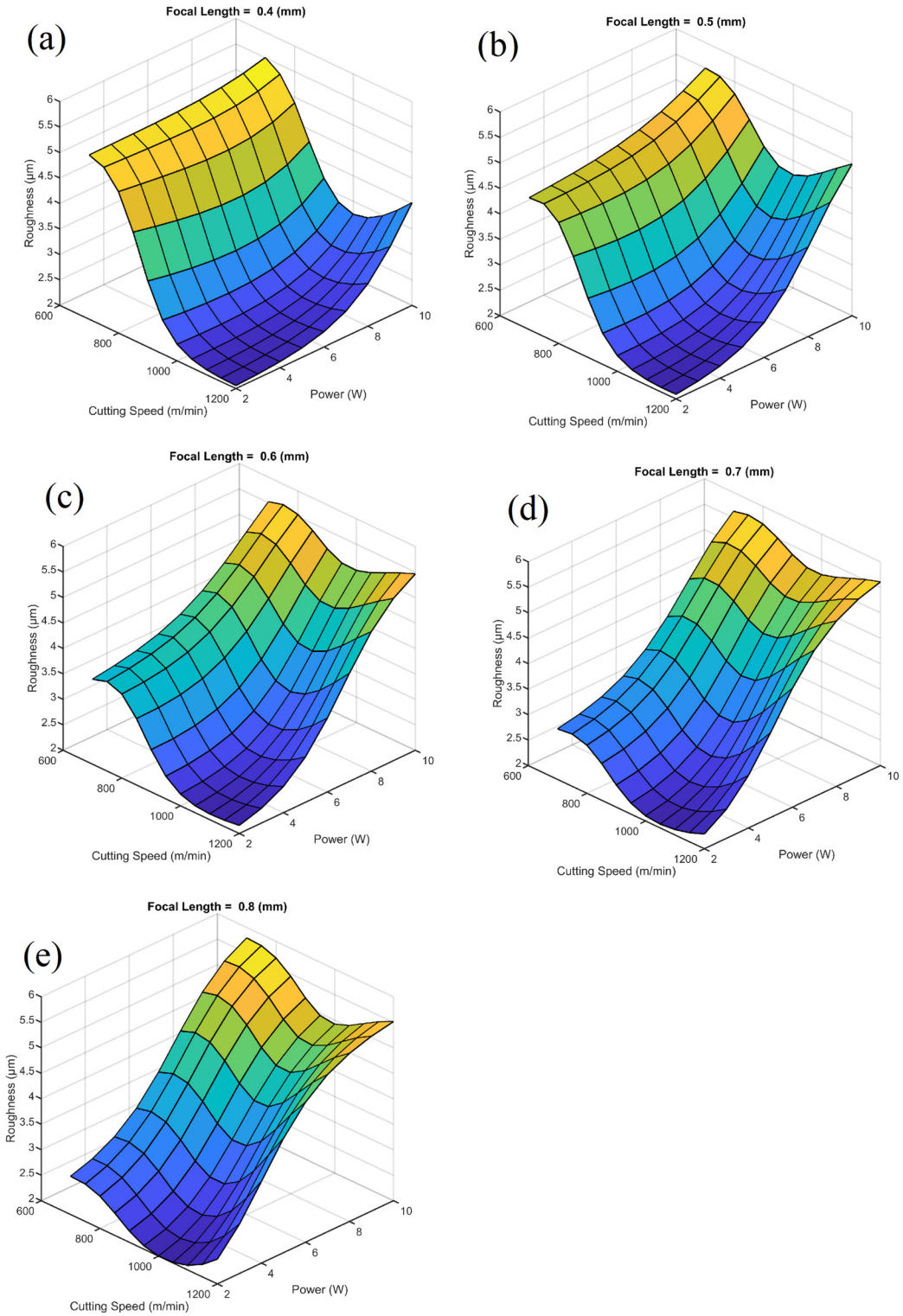

FIG. 10. The roughness for the focal length of (a) 0.4, (b) 0.5, (c) 0.6, (d) 0.7, and (e) 0.8 mm.

B. PSO technique

PSO is a powerful optimization technique derived by the social behavior of birds and insects. In PSO, a population of particles is used to explore the search space and find the optimal solution to a given problem. Individuals in a group are able to coordinate their movements to achieve a common goal.

At the start of the PSO algorithm, a particles population is randomly created. Each particle presents a potential solution to the problem being optimized. Each particle is also assigned a velocity, which determines how fast the particle moves in the search space. According to the present location of particle's and considering the best spot, it has yet looked at the algorithm updates the speed at each iteration. The best position reached by any particle in the population is referred to as the "global best," while the best position reached by any individual particle is referred to as the "personal best" of that particular particle.

The movement of the particles in the probe area is guided by two factors: their personal best position and the global best position. These factors influence the direction and speed of the particles' movement, with the goal of finding the optimal solution to the problem. In each iteration of the algorithm, the position and velocity of each particle are updated according to the following equations:

$$v_i^j(t+1) = \omega v_i^j(t) + c_1 r_1(t)(pbest_i^j - x_i^j(t)) + c_2 r_2(t)(gbest^j - x_i^j(t)), \quad (1)$$

$$x_i^j(t+1) = x_i^j(t) + v_i^j(t+1), \quad (2)$$

where $v_i^j(t)$ is the speed of particle i in iteration j at time t, $x_i^j(t)$ is the running position of particle i in iteration j at time t, $pbest_i^j$ is the personal best position of particle i in iteration j, $gbest^j$ is the global optimal position in iteration j, ω is the weight, and c_1 and c_2 are coefficients of acceleration.

r_1 and r_2 are random amounts between 0 and 1 that determine the influence of the personal proper and global proper positions on the particle's motion. The inertia weight ω determines the tradeoff between local and global discovery. A high value of ω favors global exploration, allowing the particles to move fast in the probe zone and discover new regions. A low value of ω favors local exploration, allowing the particles to converge to the best solutions found so far. The acceleration coefficients c_1 and c_2 control the influence of the global perfect and personal perfect positions on the particle's movement. A high value of c_1 favors discovery of the personal best position, while a high value of c_2 favors discovery of the global optimal position.

PSO has several advantages over other optimization algorithms: It is relatively easy to implement and can handle nonlinear and nonconvex problems with multiple optima. The PSO is also computationally efficient and can converge quickly to the optimal solution. However, PSO also has some limitations. It can be sensitive to the selection of parameters, such as the acceleration coefficients and the inertia weight. In addition, PSO may converge prematurely to a suboptimal solution if the particles become trapped in a local optimum.

The flowchart for the PSO technique is illustrated in Fig. 11.

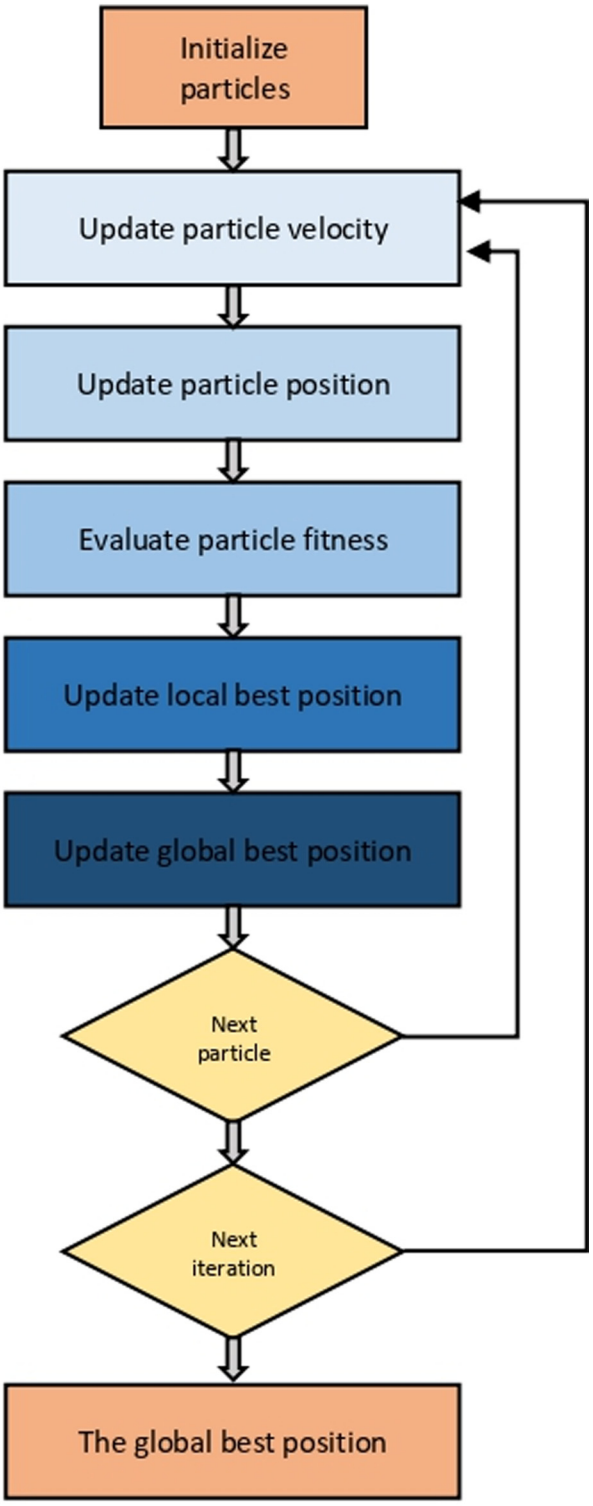

FIG. 11. The chart for the PSO technique.

C. Multiobjective PSO technique

Multiobjective PSO, a variation in the basic PSO method, is intended to address optimization issues involving multiple, opposing objectives. In multiobjective PSO, each particle's fitness is evaluated based on multiple objective functions that represent different optimization goals. To solve multiobjective problems, multiobjective PSO utilizes a concept known as Pareto dominance. A solution is said to dominate another solution if it is better than the other solution in at least one objective and not worse in any other objective. By introducing Pareto dominance and other mechanisms to facilitate exploration and exploitation of the search space, multiobjective PSO can generate a diverse set of nondominated solutions that represent trade-offs between competing objectives. The multiobjective PSO produces a set of optimal solutions that provide decision-makers with a range of trade-off options between different objectives. Multiobjective PSO also introduces new mechanisms to facilitate exploration and exploitation of the search space. One common approach is to use diversity measures to encourage particles to search for solutions in different regions of the search space.

D. Multiobjective optimization of fiber laser cutting characteristics

Selecting the optimal parameters ranges has been the main goal of this study. In this study, the minimum value of surface roughness has been the major measurement according to the interaction with other parameters. Furthermore, in most cases, the temperature higher 350 °C clearly ends in minimum roughness in case of creating a smooth cut kerf region with minimum slags. Therefore, the investigated set of parameters at lower speeds and higher laser power could produce the appropriate quality. The roughness values below 2.8 μm could be a threshold level for selecting the suitable condition. Seemingly, the parameters' interactions could have drawbacks on the resultant roughness and cut quality. Low cutting speed and very much high power can have a detrimental effect on cut quality by excessive heating and high spattering although has been a criterion on selecting the optimal parameters. Hence, the multiobjective optimization algorithm can play an important role in selecting the optimal parameters.

The maximum temperature and roughness are the objective functions. These two objectives are considered in the multiobjective optimization where the goal is to minimize both objectives simultaneously. In multiobjective optimization with two objectives, the result is often a set of solutions that lie on a Pareto optimal front. In this case, the Pareto optimal front would represent the trade-off between minimizing the maximum temperature and minimizing the roughness. The solutions on the Pareto front would be considered the best solutions since they cannot be improved in one objective without sacrificing performance in the other. The result of a Pareto optimal front can be visualized using a scatter plot, with the maximum temperature on the x-axis and the roughness on the y-axis. Each point on the plot represents a solution, and the Pareto front is the set of points that cannot be improved in one objective without sacrificing performance in the other.

The shape of the Pareto front is important because it gives insight into the nature of the trade-offs between the objectives. The Pareto optimal front is illustrated in Fig. 12. The concave Pareto front indicates that the trade-offs are almost severe.

TABLE III. Optimal independent and dependent variables.

Cutting speed (m/min)	Focal length (mm)	Power (W)	Roughness (μm)	Max. temperature (°C)
4.39	0.75	840	3.00	370
4.04	0.77	835	2.91	371
2.21	0.79	1069	2.07	409
3.42	0.79	1083	2.41	395
2.66	0.80	1081	2.18	398
3.90	0.79	1079	2.57	392
3.55	0.79	1083	2.46	394
3.63	0.79	830	2.82	372
2.05	0.79	1043	2.02	419
2.04	0.79	1018	2.01	424
3.40	0.79	831	2.76	376
3.37	0.79	837	2.73	380
2.91	0.80	1081	2.24	397
2.41	0.80	1081	2.13	400
3.05	0.78	830	2.70	383
2.27	0.79	1052	2.05	415
2.50	0.80	1059	2.10	408
4.39	0.75	840	3.00	370

The Pareto optimal front can be used to identify a solution that balances the objectives in a way that is most suitable for the problem at hand. The optimal independent and dependent variables are presented in Table III. As can be seen, there are two optimal powers of about 830 and 1080 W. The former results in lower maximum temperature and higher roughness, while the latter causes higher temperature and lower roughness. Also, the cutting

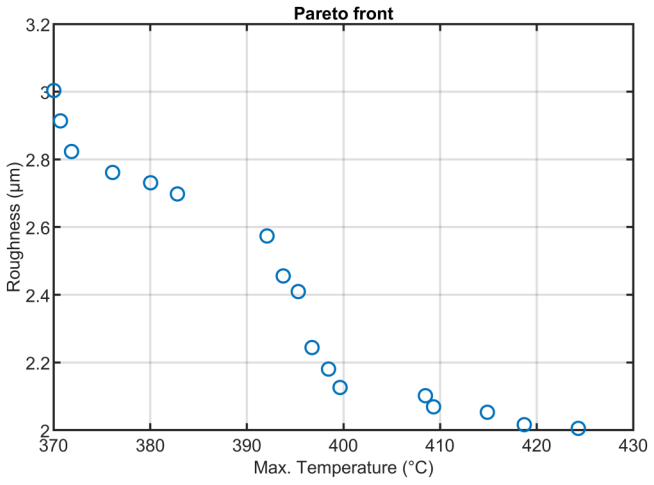

FIG. 12. The Pareto optimal front.

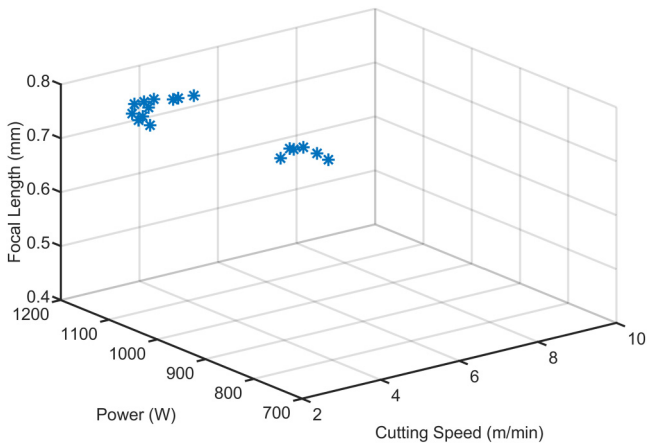

FIG. 13. The distribution of the optimal points in the input domain.

velocity ranges from 2 to 4 m/min in all the optimal cases, which is almost low in the studied range. Furthermore, in all optimal cases, the focal length is almost maximum. The distribution of the optimal points in the input domain is illustrated in Fig. 13.

V. CONCLUSION

The present study aimed to determine the impact of laser cutting measures on the temperature and surface roughness of the cutting edge of Inconel 600 sheets, utilizing the error back propagation method. The "trainbr" learning technique was chosen for network training, given its fast convergence rate. The findings of the study can be summarized as follows:

- The network architecture exhibited the lowest relative error.
- For temperature and surface roughness, the ideal number of neurons in the hidden layer was identified.
- The impressive performance of the used ANN was revealed by the high correlation R values in the training and testing phases.
- The experimental result showed that high cutting speed at low level of laser power and focal point positon at the surface of the Inconel 600 sheet produced the high roughness and low cut quality due to creating slags and incomplete melting of the materials.
- There are two optimal power of about 830 and 1080 W. The former results in lower maximum temperature and higher roughness, while the latter causes higher temperature and lower roughness.
- The cutting velocity ranges from 2 to 4 m/min in all the optimal cases, which is almost low in the studied range.
- In all optimal cases, the focal length is almost maximum in case the focal point has been located below the sheet surface at least about 1 mm.
- The temperature ranges' optimization was performed according to selecting the ranges' limit between 370 and 419 °C that completely melt the material and prevent creating defects such as dross attachment and melted material accumulation at lower part of the cut kerf.
- At laser power of 1000 W and speed of 4 m/min, the smooth cutting edge at minimum roughness was gained without any defects. At laser power of 830 W and cutting speed of 3 m/min and focal length of 0.78, the minimum roughness of 2.7 μm is gained. Hence, it can be concluded that a higher laser power level more than 1000 W can offer wider ranges of speed and focal length for selecting optimal parameters because of having more efficient melting eligibility.

AUTHOR DECLARATIONS

Conflict of Interest

The authors have no conflicts to disclose.

Author Contributions

Mohammad Hossein Razavi Dehkordi, Mohammad Akbari, and Seyed Amin Bagherzadeh conducted methodology, software, and validation. Seyed Amin Bagherzadeh, Mohammadreza Ghazi, and Mohammadkarimi conducted the experimental test and analysis of the data. Mohammad Hossein Razavi Dehkordi, Mohammad Akbari, and Seyed Amin Bagherzadeh wrote the paper.

Mohammad Hossein Razavi Dehkordi: Data curation (equal); Investigation (equal); Software (supporting). **Dheyaa J. Jasim:** Writing – review & editing (equal). **Ameer H. Al-Rubaye:** Writing – review & editing (equal). **Mohammad Akbari:** Data curation (equal); Formal analysis (equal); Project administration (supporting); Supervision (lead); Writing – original draft (equal). **Seyed Amin Bagherzadeh:** Software (lead); Validation (equal); Writing – original draft (equal). **Mohammadreza Ghazi:** Conceptualization (equal); Resources (equal). **Hamed Mohammadkarimi:** Methodology (equal); Project administration (equal).

DATA AVAILABILITY

The raw/processed data required to reproduce these findings cannot be shared at this time due to technical or time limitations.

REFERENCES

[1]L. Wang and Y. Rong, "Review on processing stability, weld defects, finite element analysis, and field assisted welding of ultra-high-power laser (≥10 kW) welding," Int. J. Hydromechatronics **5**, 167–190 (2022).
[2]M. J. H. Rawa, M. H. R. Dehkordi, M. J. Kholoud, N. H. Abu-Hamdeh, and H. Azimy, "Using the numerical simulation and artificial neural network (ANN) to evaluate temperature distribution in pulsed laser welding of different alloys," Eng. Appl. Artif. Intell. **126**, 107025 (2023).
[3]N. Erum and J. Ahmad, "Structural, elastic and mechanical properties of cubic perovskite materials," Arch. Adv. Eng. Sci. **2023**, 1–6 (2023).
[4]S. Stoyanov, D. Petring, D. Arntz-Schroeder, M. Günder, A. Gillner, and R. Poprawe, "Investigation on the melt ejection and burr formation during laser fusion cutting of stainless steel," J. Laser Appl. **32**, 022068 (2020).
[5]D. Arntz, D. Petring, U. Jansen, and R. Poprawe, "Advanced trim-cut technique to visualize melt flow dynamics inside laser cutting kerfs," J. Laser Appl. **29**, 022213 (2017).

[6]Y. Yongbin, S. A. Bagherzadeh, H. Azimy, M. Akbari, and A. Karimipour, "Comparison of the artificial neural network model prediction and the experimental results for cutting region temperature and surface roughness in laser cutting of AL6061T6 alloy," Infrared Phys. Technol. **108**, 103364 (2020).
[7]M. Sharifi and M. Akbari, "Experimental investigation of the effect of process parameters on cutting region temperature and cutting edge quality in laser cutting of AL6061T6 alloy," Optik **184**, 457–463 (2019).
[8]M. Schleier, B. Adelmann, C. Esen, U. Glatzel, and R. Hellmann, "Development and evaluation of an image processing algorithm for monitoring fiber laser fusion cutting by a high-speed camera," J. Laser Appl. **33**, 032004 (2021).
[9]J. Pocorni, J. Powell, J. Frostevarg, and A. F. H. Kaplan, "Investigation of the piercing process in laser cutting of stainless steel," J. Laser Appl. **29**, 022201 (2017).
[10]M. Azari, E. Rasti, M. H. R. Dehkordi, H. Azimy, A. Zarei, and S. A. Bagherzadeh, "Investigation of temperature distribution and melt pool microstructure in laser fusion welding of inconel 625 superalloy," J. Laser Appl. **33**, 022015 (2021).
[11]J. Wang, Z. Sun, L. Gu, and H. Azimy, "Investigating the effect of laser cutting parameters on the cut quality of inconel 625 using response surface method (RSM)," Infrared Phys. Technol. **118**, 103866 (2021).
[12]P. A. Hilton, D. Lloyd, and J. R. Tyrer, "Use of a diffractive optic for high power laser cutting," J. Laser Appl. **28**, 012014 (2016).
[13]Y. Peng, Milad Boroumand Ghahnaviyeh, Mohammad Nazir Ahmad, Ali Abdollahi, Seyed Amin Bagherzadeh, Hamidreza Azimy, Amirhosein Mosavi, and Aliakbar Karimipour, "Analysis of the effect of roughness and concentration of Fe3O4/water nanofluid on the boiling heat transfer using the artificial neural network: An experimental and numerical study," Int. J. Therm. Sci. **163**, 106863 (2021).
[14]X. Dong, W. Hao, J. Liu, G. Wang, and H. Ren, "Effect of laser parameters on melting ratio and temperature distribution in dissimilar laser welding of brass and SS 308 using the artificial neural network model," J. Laser Appl. **33**, 032003 (2021).
[15]G. Norkey, K. Pratap Singh, A. Prajapati, and V. Sharma, "Intelligent parameters optimization for laser cutting of highly reflective and thermally conductive materials using artificial neural network," Mater. Today **46**, 4757–4764 (2021).
[16]C. Sun, M. H. R. Dehkordi, M. J. Kholoud, H. Azimy, and Z. Li, "Systematic evaluation of pulsed laser parameters effect on temperature distribution in dissimilar laser welding: A numerical simulation and artificial neural network," Opt. Laser Technol. **163**, 109407 (2023).
[17]N. Luo, Hua Yu, Zeqing You, Yao Li, Tunan Zhou, Nan Han, Chenxu Liu, Zihan Jiang, and Shaojie Qiao, "Fuzzy logic and neural network-based risk assessment model for import and export enterprises: A review," J. Data Sci. Intell. Syst. **1**(1), 2-11 (2023).
[18]Z. Li and S. Li, "Recursive recurrent neural network: A novel model for manipulator control with different levels of physical constraints," CAAI Trans. Intell. Technol. **8**(3), 622–634 (2023).
[19]Q. Zhang, Jingyu Xiao, Chunwei Tian, Jerry Chun-Wei Lin, and Shichao Zhang, "A robust deformed convolutional neural network (CNN) for image denoising," CAAI Trans. Intell. Technol. **8**(2), 331–342 (2023).
[20]H. Taherdoost and M. Madanchian, "Analytic network process (ANP) method: A comprehensive review of applications, advantages, and limitations," J. Data Sci. Intell. Syst. **1**(1), 12–18 (2023).
[21]N. T. K. Chi and N. Hoang Vu, "Investigating the customer trust in artificial intelligence: The role of anthropomorphism, empathy response and interaction," CAAI Trans. Intell. Technol. **8**(1), 260–273 (2023).
[22]Z. Chen, "Research on internet security situation awareness prediction technology based on improved RBF neural network algorithm," J. Comput. Cogn. Eng. **1**(3), 103–108 (2022).
[23]M. Asmael and A. Memarzadeh, "A review on recent achievements and challenges in electrochemical machining of tungsten carbide," Arch. Adv. Eng. Sci. **2023**, 1–23 (2023).
[24]Y. Guo, Z. Mustafaoglu, and D. Koundal, "Spam detection using bidirectional transformers and machine learning classifier algorithms," J. Comput. Cogn. Eng. **2**(1), 5–9 (2022).
[25]B. K. Liu and W. Z. Lu, "Surrogate models in machine learning for computational stochastic multi-scale modelling in composite materials design," Int. J. Hydromechatronics **5**, 336–365 (2022).
[26]S. Saminu, Guizhi Xu, Shuai Zhang, Isselmou Ab El Kader, Hajara Abdulkarim Aliyu, Adamu Halilu Jabire, Yusuf Kola Ahmed, and Mohammed Jajere Adamu, "Applications of artificial intelligence in automatic detection of epileptic seizures using EEG signals: A review," Artifi. Intell. Appl. **1**, 11–25 (2023).
[27]O. Shekoofa, J. Wang, and D. Li, "Fabrication of n-type nanocrystalline silicon thin-film by magnetron sputtering and antimony induced crystallization," Arch. Adv. Eng. Sci. **2023**, 1–11 (2023).
[28]T. Tyagi, S. Kumar, A. K. Malik, and V. Vashisth, "A novel neuro-optimization technique for inventory models in manufacturing sectors," J. Comput. Cogn. Eng. **2**(3), 204–209 (2022).
[29]L. Gang, G. Huang, H. Yuan, S. Xia, and W. Tan, "Analysis and optimisation of impact wear of diesel engine needle valve assembly," Int. J. Hydromechatronics **5**, 80–91 (2022).
[30]N. Roy, D. Pramanik, and A. S. Kuar, "Comparative study on quality characteristic of pulsed laser beam cutting of inconel 625 superalloy at different environment by sensitivity analysis," Optik **232**, 166516 (2021).
[31]P. K. Shrivastava, B. Singh, and Y. Shrivastava, "Prediction of optimal cut quality characteristic of inconel 718 sheet by genetic algorithm and particle swarm optimization," J. Laser Appl. **31**, 022016 (2019).
[32]S. Vagheesan and J. Govindarajalu, "Hybrid neural network–particle swarm optimization algorithm and neural network–genetic algorithm for the optimization of quality characteristics during CO2 laser cutting of aluminium alloy," J. Braz. Soc. Mech. Sci. Eng. **41**, 328 (2019).
[33]P. Kumar Shrivastava, G. Norkey, and A. Kumar Pandey, "Optimization of process parameters during the laser cutting of inconel-718 sheet using regression based genetic algorithm," Mater. Today Proc. **18**, A17–A25 (2019).
[34]S. Chaki, R. N. Bathe, S. Ghosal, and G. Padmanabham, "Multi-objective optimisation of pulsed Nd:YAG laser cutting process using integrated ANN–NSGAII model," J. Intell. Manuf. **29**, 175–190 (2018).
[35]N. Roy, A. Kuar, S. Mitra, and A. Das, "Sensitivity analysis of process parameters in submerged laser beam cutting on Inconel 625 superalloy," in *International Conference on Precision, Meso, Micro and Nano Engineering*, India (2017), Vol. 10, pp. 247–250.
[36]N. Roy, A. Kuar, S. Mitra, and A. Das, "Submerged pulsed Nd: YAG laser beam cutting of inconel 625 superalloy: Experimental investigation," Lasers Eng. **35**, 151–171 (2016).
[37]J. Wei, Y. Ye, Z. Sun, L. Liu, and G. Zou, "Control of the kerf size and microstructure in inconel 738 superalloy by femtosecond laser beam cutting," Appl. Surf. Sci. **370**, 364–372 (2016).
[38]F. Jafarian and A. Barghak, "Experimental investigations in order to evaluate the kerf and surface roughness in the laser cutting process of Inconel 718 superalloy and process optimization," Modares Mech. Eng. **15**(13), 68–72 (2016).
[39]H. Tebassi, M. A. Yallese, I. Meddour, F. Girardin, and T. Mabrouki, "On the modeling of surface roughness and cutting force when turning of inconel 718 using artificial neural network and response surface methodology: Accuracy and benefit," Periodica Polytech Mech. Eng. **61**, 1–11 (2017).
[40]Y. Nukman, M. Hassan, and M. Harizam, "Optimization of prediction error in CO2 laser cutting process by taguchi artificial neural network hybrid with genetic algorithm," Appl. Math. Inf. Sci. **7**, 363–370 (2013).
[41]M. Grepl, J. Petru, R. Cep, L. Petrkovska, and T. Zlamal, "The effect of process parameters on result quality of cut during laser cutting of material," in *Proceedings of the 23th DAAAM International Symposium, ISSN*, Annals of DAAAM for 2012 & Proceedings of the 23rd International DAAAM Symposium, Vienna, Austria (2012), Vol. 23041382, pp. 1035–1038.

[42]M. Madić and M. Radovanović, "Comparative modeling of CO2 laser cutting using multiple regression analysis and artificial neural network," Int. J. Physic. Sci. **7**(16), 2422–2430 (2012).
[43]C.-B. Yang, C.-S. Deng, and H.-L. Chiang, "Combining the taguchi method with artificial neural network to construct a prediction model of a CO2 laser cutting experiment," Int. J. Adv. Manuf. Technol. **59**, 1103–1111 (2012).
[44]M.-J. Tsai, C.-H. Li, and C.-C. Chen, "Optimal laser-cutting parameters for QFN packages by utilizing artificial neural networks and genetic algorithm," J. Mater. Proc. Technol. **208**, 270–283 (2008).
[45]D. Pramanik, N. Roy, A. S. Kuar, S. Sarkar, and S. Mitra, "Experimental investigation of sawing approach of low power fiber laser cutting of titanium alloy using particle swarm optimization technique," Opt. Laser Technol. **147**, 107613 (2022).
[46]S. Chaki, D. Bose, and R. N. Bathe, "Multi-objective optimization of pulsed Nd: YAG laser cutting process using entropy-based ANN-PSO model," Lasers Manuf. Mater. Proc. **7**, 88–110 (2020).
[47]P. K. Shrivastava, B. Singh, and Y. Shrivastava, "Prediction of optimal cut quality characteristic of inconel 718 sheet by genetic algorithm and particle swarm optimization," J. Laser Appl. **31**, 022016 (2019).